ARTICLE
Journal of Cellular Biochemistry 114:2795–2808 (2013)

Journal of Cellular Biochemistry

Comparative Proteomics of Glioma Stem Cells and Differentiated Tumor Cells Identifies S100A9 as a Potential Therapeutic Target

Song Chen, Hongxin Zhao, Jinmu Deng, Peng Liao, Zhongye Xu, and Yuan Cheng*

Department of Neurosurgery, The Second Affiliated Hospital, Chongqing Medical University, Chongqing, China

ABSTRACT

Recent studies have suggested the existence of a small subset of cancer cells called cancer stem cells (CSCs), which possess the ability to initiate malignancies, promote tumor formation, drive metastasis, and evade conventional chemotherapies. Elucidation of the specific signaling pathway and mechanism underlying the action of CSCs might improve the efficacy of cancer treatments. In this study, we analyzed differentially expressed proteins between glioma stem cells and differentiated tumor cells isolated from the human glioma cell line, U251, via iTRAQ-tagging combined with two dimensional liquid chromatography tandem MS analysis to identify proteins correlated with specific features of CSCs. Out of a total data set of 559 identified proteins, 29 proteins were up-regulated in the glioma stem cells when compared with the differentiated cells. Interestingly, The expression level of S100A9 was fivefold higher in glioma stem cells than differentiated cells. Similar results were also observed in glioma stem cells derived from other glioma cells. More importantly, knockdown of S100A9 by RNA interference suppressed the proliferation of glioma stem cell line and decreased the growth of xenograft tumors in vivo. Taken together, these results indicate that the tumorigenesis potential of CSCs arises from highly expressed S100A9. J. Cell. Biochem. 114: 2795–2808, 2013.

KEY WORDS: S100A9; GLIOMA STEM CELLS; GLIOMA; iTRAQ; PROLIFERATION; TUMORIGENESIS

Gliomas are the most malignant primary brain tumor. Malignant gliomas are among the most devastating and lethal cancers. Despite aggressive treatment approaches, the therapeutics of gliomas is still poor, with the median survival time remains less than 1 year [Ohgaki et al., 2004]. The poor survival is primarily because of the recurrence of tumor and resistant to standard therapies [Reardon et al., 2006]. Therefore, new strategies to treat malignant gliomas are urgently needed.

There is increasing evidence that a small population of cancer stem cells (CSCs) within solid tumors is responsible for tumor formation and ongoing growth [Reya et al., 2001; Visvader and Lindeman, 2008]. The existence of CSCs has been demonstrated in GBMs [Galli et al., 2004; Singh et al., 2004]. These CSCs share similar properties with normal stem cells and have the ability to self-renew, differentiate and drive tumorigenesis. The CSCs are resistant to radiation therapy [Bao et al., 2006] and chemotherapy [Liu et al., 2006], and are considered to be the most likely cause of cancer recurrence. It should be noted that recent findings have shown the possibility of targeting CSCs for the treatment of brain tumors [Piccirillo et al., 2006; Li et al., 2009a; Fan et al., 2010; Eyler et al., 2011; Guryanova et al., 2011; Zhu et al., 2011]. Discovery of potential therapeutic markers for CSCs is the intense interest.

Quantitative protein expression profiling allows efficient identification of accurate and reproducible differential expression values for proteins in multiple biological samples. Comparison of protein expression profiles between tumors and normal tissues and among different tumors may lead to discovery of disease specific targets and biomarkers, and elucidation of molecular mechanisms. Isobaric tags for relative and absolute quantitation (iTRAQ) combined with multidimensional liquid chromatography (LC) and tandem MS analysis is emerging as a powerful methodology in the search for tumor biomarkers [Ross et al., 2004; Chaerkady et al., 2008; Eriksson

Abbreviations: iTRAQ, isobaric tags for relative and absolute quantitation; LC-ESI-MS/MS, liquid chromatography-electrospray ionization-tandem mass spectrometry; MMTS, methyl methanethiosulfonate.

All authors have no conflict of interests.

Grant sponsor: National Natural Science Foundation of China; Grant number: 30801348 30870723; Grant sponsor: Program for Changjiang Scholars; Grant sponsor: Innovative Research Team; Grant numbers: IRT, 0872.

*Correspondence to: Yuan Cheng, Department of Neurosurgery, The Second Affiliated Hospital, Chongqing Medical University, 74 Linjiang Rd, Yuzhong 400010, Chongqing, China. E-mail: chengyuan023@yahoo.com.cn

Manuscript Received: 6 April 2013; Manuscript Accepted: 27 June 2013

Accepted manuscript online in Wiley Online Library (wileyonlinelibrary.com): 8 July 2013

DOI 10.1002/jcb.24626 • © 2013 Wiley Periodicals, Inc.

et al., 2008; Glen et al., 2008; Pierce et al., 2008; Bijian et al., 2009; Bouchal et al., 2009]. In this study, we describe a quantitative proteomics analysis of glioma stem cells and differentiated tumor cells using iTRAQ labeling followed by 2D LC–MS/MS approach. To the best of our knowledge, the iTRAQ strategy has not been reported to date in glioma stem cell.

Notwithstanding the fact that gliomas are highly heterogeneous, we anticipated that the list of proteins aberrantly expressed within this 2-cell line model would reflect at least some of the types of clinical gliomas and serve as a useful reference for future basic or translational cancer research. S100A9 was identified as being up regulated in the glioma stem cell in this study. Its role and mode of action in glioma cell proliferation and growth were investigated.

MATERIALS AND METHODS

CELL CULTURE

U251, SHG44, and U87 cells was obtained from the American Type Culture Collection (ATCC, Manassas, VA, USA) and cultured in DMEM supplemented with 10% fetal bovine serum, 100 U/ml penicillin and 100 U/ml streptomycin in a 5% CO_2 atmosphere. Glioma stem cells were cultured in SFM (serum-free medium) supplemented with DMEM/F12, 20 ng/ml basic fibroblast growth factor (bFGF), 20 ng/ml epidermal growth factor (EGF), 20 μl/ml B27 supplement, and 10 ng/ml leukemia inhibitory factor (LIF).

MAGNETIC CELL SORTING (MACS)

Cells were labeled with primary CD133/1-PE antibody (Miltenyi Biotec), then labeled with anti-PE microbeads (Miltenyi Biotec), and isolated on a MACS LS column (Miltenyi Biotec). All procedures were performed according to the manufacturer's instructions. Isotype-matched mouse immunoglobulins (Miltenyi Biotec) served as controls. The purity of sorted cells was evaluated by flow cytometry and immunofluorescent staining. Flow cytometry was done using a FACScan (BD Biosciences). Data were analyzed by BD FACS datafiles software, which is provided with the system.

FLUORESCENCE ACTIVATED CELL SORTING (FACS)

Cells were labeled with primary CD133/1-PE antibody (Miltenyi Biotec). All procedures were performed according to the manufacturer's instructions. Isotype-matched mouse immunoglobulins (Miltenyi Biotec) served as controls. Cells were sorted by using a FACScan. Data were analyzed by BD FACS datafiles software, which is provided with the system.

IMMUNOFLUORESCENT STAINING

The tumor spheres were pre-incubated in DMEM plus 10% FBS for 4 h in order to attach the coverslips which were coated by polylysine. The cells were fixed by paraform for 30 min and were washed by PBS again three times. After blocked by 5% goat serum at 37°C for 30 min. The colonies were labeled with CD133 antibody (1:100 dilution, mouse monoclonal, Santa Cruz, CA, USA), nestin antibody (1:100 dilution, rabbit monoclonal, Santa Cruz, CA, USA) at 4°C overnight. Then the second antibody, Cy3-conjugated goat anti-mouse IgG (1:100 dilution, BioLegend), and FITC-conjugated goat anti- rabbit IgG was added and incubated at 37°C for 1 h. For assessment of the differentiation of those tumor spheres, GFAP (Glial fibrillary acidic protein) (1:100 dilution, goat anti-human ploy clonal, SantaCruz, CA, USA) used for incubation of these cells, and the appropriate second antibodies were employed as described above, Nuclei were stained with 50 ng/ml 4′,6-diamidine-2-phenylindole dilactate (DAPI) for 5 min at room temperature then detected by a laser confocal microscope(LeicaSP-5, Germany).

SAMPLE PREPARATION

Glioma stem cell and differentiated tumor cell cultures were seeded in 10 cm^2 diameter tissue culture plates and cultured for 24 h in serum-free stem cell medium. Cells were subsequently washed twice with phosphate-buffered saline, centrifuged, and washed with water to get rid of the excess salts. Lysis buffer (20 mM HEPES pH7.4, 1% Nonidet P-40, 150 mM NaCl, 5 mM $MgCl_2$, 10% glycerol) containing proteinase inhibitor was used to lyse cells. The concentration of proteins was determined using 2D Quantification kit (Amersham Biosciences, Uppsala, Sweden).

PROTEIN DIGESTION AND LABELING WITH ITRAQ REAGENTS

Trypsin digestion and iTRAQ labeling were performed according to the manufacturer's protocol (Applied Biosystems, Framingham, MA). Briefly, From each cell lines, 100 μg of proteins were evaporated to dryness and dissolved in the solution buffer, denatured, and then cysteines were blocked. Each sample was digested with 20 μl of 0.1 μg/μl trypsin (mass spectrometry grade; Promega, Madison, WI) solution at 37°C overnight and then labeled with the iTRAQ reagents (Applied Biosystems) as follows: (i) glioma cell—113 tag, (ii) Stem cell —114, (iii) Glioma cell—115 tags, and (IV) Stem cell—116. The labeled samples were pooled prior to further analysis.

ON-LINE 2D LC

The mixed peptides were fractionated by strong cation exchange chromatography on a 20AD HPLC system (Shimadzu) using a polysulfoethyl column (2.1 × 100 mm, 5 μm, 300 Å; The MD Inc.) as previously described. Briefly, the mixed peptides were desalted with Sep-Pak Cartridge (Waters, Milford, MA), diluted with the loading buffer (10 mM KH_2PO_4 in 25% acetonitrile, pH 2.6) and loaded onto the column. Buffer A was identical in composition to the loading buffer, and buffer B was same as buffer A except containing 500 mM KCl. Separation was performed using a linear binary gradient of 0–80% buffer B in buffer A at a flow rate of 200 μl/min for 60 min.

Each strong cation exchange fraction was dried down, dissolved in buffer C (5% acetonitrile, 0.1% formic acid), and analyzed on Qstar XL (Applied Biosystems) as previously described. Briefly, peptides were separated on a reverse-phase (RB) column (ZORBAX 300SB-C18 column, 5 μm, 300 Å, 0.1 × 15 mm; Microm) using a 20AD HPLC system (Shimadzu). The HPLC gradient was 5–35% buffer D (95% acetonitrile, 0.1% formic acid) in buffer C at a flow rate of 200 μl/min for 65 min. Survey scans were acquired from 400–1,800 with up to four precursors selected for MS/MS from m/z 100–2,000 using a dynamic exclusion of 30S. The iTRAQ labeled peptides fragmented under collision-induced dissociation conditions to give reporter ions at 113.1, 114.1, 115.1, and 116.1 Th. The ratios of peak areas of the iTRAQ reporter ions reflect the relative abundances of the peptides and, consequently, the proteins in the samples. Larger, sequence-

information-rich fragment ions were also produced under these MS/MS conditions and gave the identity of the protein from which the peptide originated.

DATA ANALYSIS

The software used for data acquisition was Analyst QS 1.1(Applied Biosystems). The software used for protein identification and quantitation was ProteinPilot 2.0 (Applied Biosystems) with the integrated Paragon™ search algorithm and Pro Group™ algorithm (Applied Biosystems). The protein confidence threshold cutoff is 1.3 (unused ProtScore) with at least one peptide with 95% confidence. All peptides used for the calculation of protein ratios were unique to the given protein or proteins within the group, and peptides that were common to other isoforms or proteins of the same family were ignored. The software compares relative intensity of proteins present in samples based on the intensity of reporter ions released from each labeled peptide, and automatically calculates protein ratios and *P*-values for each protein. The average iTRAQ ratios from the two 2D LC–MS/MS analyses (four iTRAQ ratios) were calculated for each protein, and significant differences in protein expression levels were determined by Student's *t*-test with a set value of $P < 0.05$.

WESTERN BLOTTING

Lysates of glioma stem cell and their differentiated offspring were prepared in lysis buffer (20 Mm HEPES pH7.4, 1% Nonidet P-40, 150 mM NaCl, 5 mM $MgCl_2$, 10% glycerol). The protein samples (about 30 μg) were separated by SDS-PAGE. After SDS-PAGE, proteins were transferred to PVDF membranes. The membranes were blocked 1 h with 1% BSA in TBS-T buffer (20 mmol/L Tris, pH 7.6, 100 mmol/L $NaCl_2$, 0.5% Tween-20), followed by overnight of incubation with the primary antibodies (1: 500 dilution), at 4°C, including monoclonal and polyclonal antibodies against S100A9, ATPA1, HSP90B1, CD44, and VIMENTIN, in TBS-T buffer containing 1% BSA at room temperature. After washing three times with TBS-T buffer, the membranes were incubated with a horseradish peroxidase-conjugated goat anti-mouse IgG, goat anti-rabbit IgG, or rabbit anti-goat IgG as a secondary antibody (1:5,000 dilution) for 1 h at room temperature. After the membranes were washed three times in TBS-T buffer, the reactions were visualized with ECL detection system. All Western blot analyses were repeated at least three times.

REAL TIME QUANTITATIVE PCR

Total RNA was isolated with the TRIzol method (Invitrogen). The first strand cDNA was synthesized from 1 ug of total RNA using reagents from Takara. Real time PCR (Bio-Rad) was performed using custom SYBR assays (Takara) following the manufacturer's instructions. The specific primers for ATP1A1 were 5′-TGCCCTGGA-ATGGGTGTTGCT-3′ (forward) and 5′-TTCTCCACCCAGCCGCCAGG-3′ (reverse), for PGK1 they were 5′-GCGACCCTTCCTGGCCATCC-3′ (forward) and 5′-TGCCAATCTCCATGTTGTTGAGCAC-3′ (reverse), for S100A9 they were 5-TGGCTCCTCGGCTTTGACAGAGT-3 (forward) and 5′-TGGGTGCCCCAGCTTCACAGA-3′ (reverse), for CD44 they were 5′-ATCGGATTTGAGACCTGCAGTTTGC-3′ (forward) and 5′-AGACTTGCTGGCCTCTCCGTTGA-3′ (reverse), for HSPB1 they were 5′-CTCAGCAGCGGGGTCTCGGA-3′ (forward) and 5′-TCGTGCTTG-CCGGTGATCTCC-3′ (reverse), and for PPIA they were 5′-TGGGCC-GCGTCTCCTTTGAG-3′ (forward) and 5′-GTCACCACCCTGACACA-TAAACCCT-3′ (reverse). We used 18s RNA as an internal control. All PCRs were performed in triplicate.

LENTIVIRAL CONSTRUCTS AND TRANSDUCTION

Knockdown of S100A9 was achieved through the use of lentiviral vector–mediated short hairpin RNA (shRNA) interference using Mission RNAi system clones (Sigma–Aldrich). S100A9-targeting lentivirus and the nontargeting control lentivirus were produced in HEK293FT cells with the ViraPower Lentiviral Expression System (Invitrogen). Three different shRNA clones were characterized in terms of knockdown efficiency using S100A9 immunoblotting of glioma stem cells infected with lentiviruses encoding S100A9 shRNA or a nontargeting control shRNA. The most efficient clone was used for all further experiments. Produced lentiviruses were concentrated by using Centricon Plus-20 centrifugal filter device (Millipore). To ensure the same number of S100A9-targeting and the control lentiviruses were used in the same experiment, produced lentiviral stock was titered and stored according to the manufacturers instruction (Invitrogen). For in vitro infection of

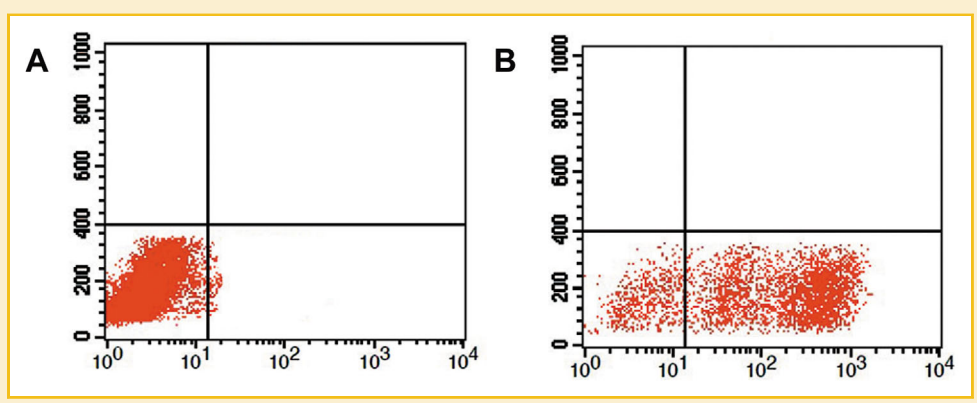

Fig. 1. A: The ratio of CD133-positive GSCs in glioma cell line U251 was determined using flow cytometry (FCM). A: The control group incubated with isotype control antibody. B: Experimental group incubated with CD133-PE.

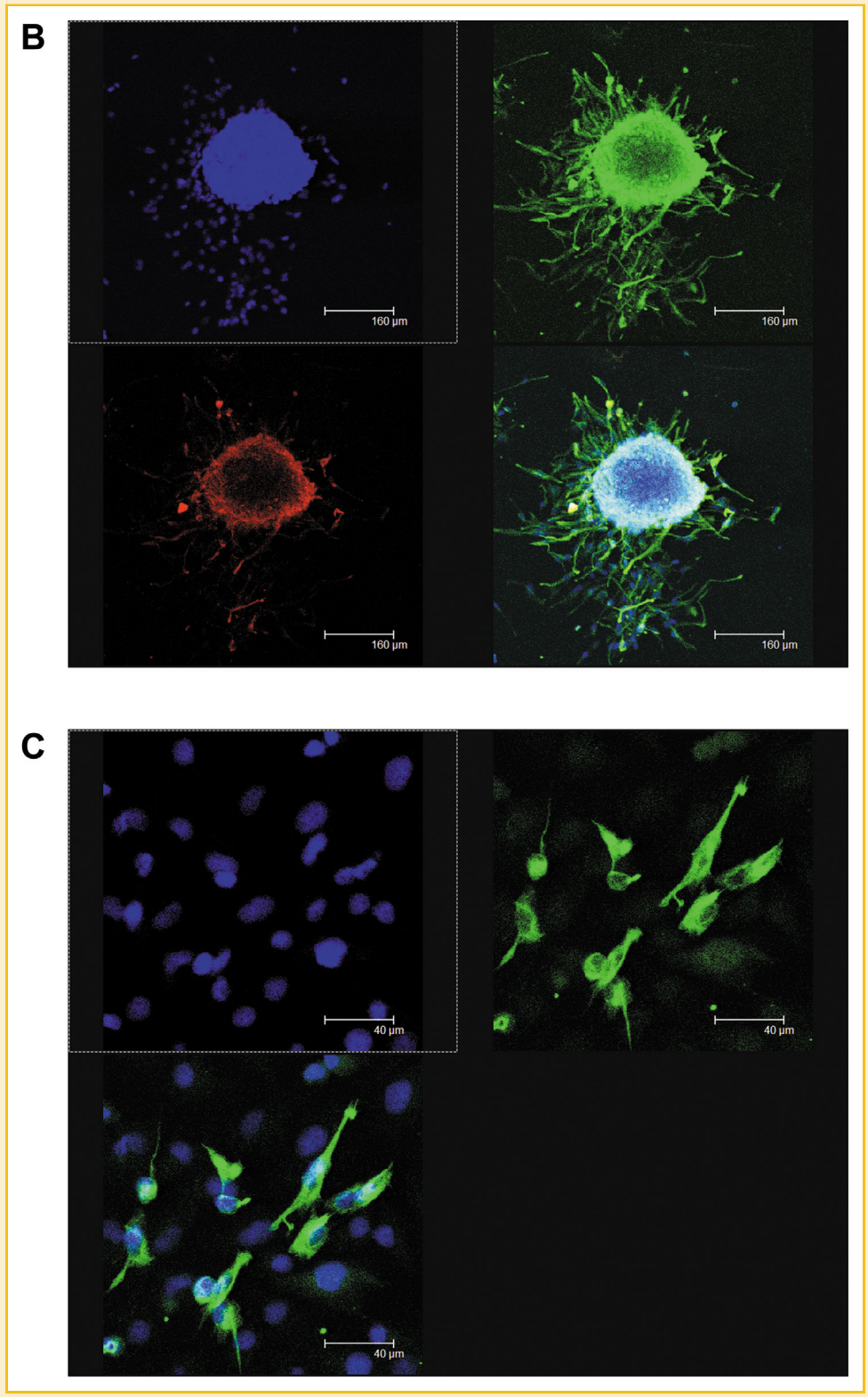

Fig. 1 Continued. B: Immunofluorescent staining of glioma stem cell spheres for CD133 (red), nestin (green), and Nuclei (blue). C: GFAP immunofluorescent staining in differentiated glioma stem cells.

glioma stem cells with the lentivirus, cultured neurospheres were disaggregated before infection to increase the infection efficiency and uniformity.

CCK-8 ASSAY

In vitro proliferation of the transfected cells was measured using CCK-8 (Cell Counting Kit-8) assay. U251 and SHG44 glioma stem cells transfected with lentivirus expressing nontargeting shRNA (sh-NC) or S100A9-targeting shRNA (sh-S100A9-1) for 48 h were plated at a density of 1,000 cells/well onto 96-well plates. For 7 days, cell viability was measured using CCK-8 (Sigma, MO, USA) and quantified by Bio-Tek Instruments EL310 Microplate Autoreader every day.

IN VIVO TUMORIGENESIS

U251 and SHG44 glioma stem cells transfected with lentivirus expressing nontargeting shRNA or S100A9-targeting shRNA were suspended in PBS and then injected subcutaneously in the right flank of athymic nude mice (2×10^6 cells/mouse, five mice/group). Tumor growth curve was plotted by means of tumor volumes monitored at indicated times. Tumor volume was calculated according to the following formula: length $\times$ (width)^2/2. The mice

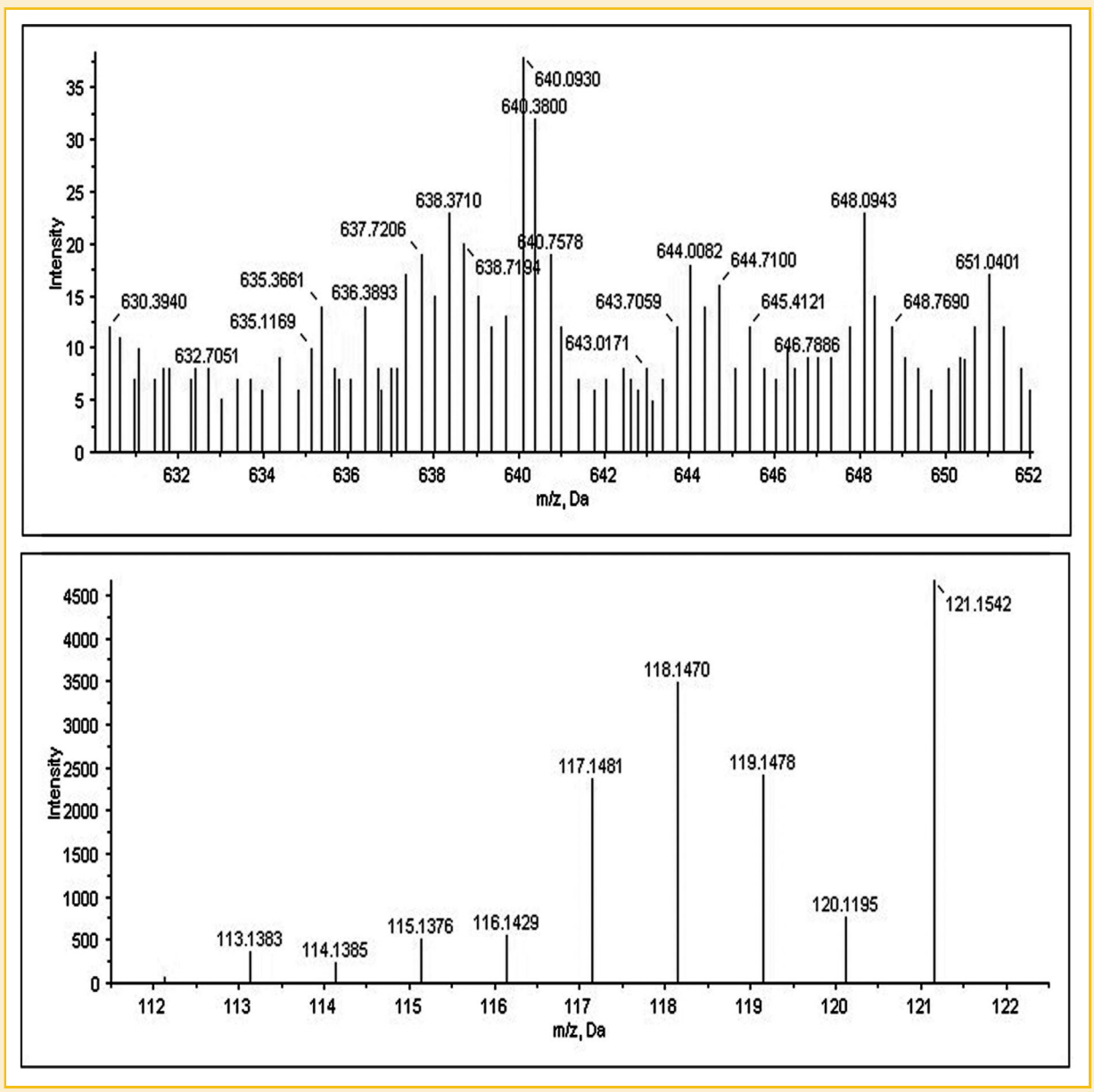

Fig. 2. A representative MS/MS spectrum showing the peptides from S100A9. U251 glioma cell were labeled with iTRAQ 113 and 115 tags, and U251 stem cell were labeled with iTRAQ 114 and 116 tags. Thus The 114:113 and 116:115 ratios indicate the relative abundance of the proteins from the stem cell line compared to the differentiated progeny.

TABLE I. iTRAQ Analysis of Differentially Expressed Proteins Between Glioma Stem Cells and the Differentiated Cells

N	Accession	Gene Sym	Protein	Stem cell: Glioma	PVal Stem cell: Glioma	Subcellular location
1	IPI:IPI00169383.3	PGK1	Poglycerate kinase 1	0.33	4.99E−03	Cytoplasm
2	IPI:IPI00853547.1	G6PD	Isoform 3 of Glucose-6-phosphate 1-dehydrogenase	0.33	2.83E−03	Cytoplasm
3	IPI:IPI00419585.9	PPIA	Peptidyl-prolyl *cis–trans* isomerase A	0.39	1.53E−06	Cytoplasm
4	IPI:IPI00003362.2	HSPA5	HSPA5 protein	0.40	8.03E−15	Endoplasmic reticulum
5	IPI:IPI00009342.1	IQGAP1	Ras GTPase-activating-like protein IQGAP1	0.55	2.41E−02	Cytoskeleton
6	IPI:IPI00376005.2	EIF5A	Isoform 2 of Eukaryotic translation initiation factor 5A-1	0.46	4.05E−02	Nucleus
7	IPI:IPI00792410.1	RPL38	8 kDa Protein	0.49	2.32E−03	Ribosome
8	IPI:IPI00025512.2	HSPB1	Heat shock protein beta-1	0.53	1.56E−05	Cytoplasm
9	IPI:IPI00023673.1	LGALS3BP	Galectin-3-binding protein	0.45	1.98E−02	Extracellular matrix
10	IPI:IPI00219018.7	GAPDH	Glyceraldehyde-3-phosphate dehydrogenase	0.68	8.30E−03	Cytoplasm
11	IPI:IPI00027230.3	HSP90B1	Endoplasmin	0.53	2.99E−05	Endoplasmic Reticulum
12	IPI:IPI00794659.1	RPS20	Ribosomal protein S20 isoform 1	0.38	3.41E−04	Ribosome
13	IPI:IPI00909207.1	PRDX2	cDNA FLJ60461, highly similar to Peroxiredoxin-2	0.54	1.93E−02	Mitochondrial
14	IPI:IPI00396485.3	EEF1A1	Elongation factor 1-alpha 1	0.54	4.55E−04	Nucleus
15	IPI:IPI00000877.1	HYOU1	Hypoxia up-regulated protein 1	0.55	9.92E−03	Endoplasmic reticulum
16	IPI:IPI00644171.1	RPL17	Putative uncharacterized protein RPL17P9	0.54	2.07E−03	Ribosome
17	IPI:IPI00025491.1	SNORA67	EIF4A1 Eukaryotic initiation factor 4A-I	0.56	4.71E−02	Nucleus
18	IPI:IPI00010204.1	SFRS3	Splicing factor, arginine/serine-rich 3	0.60	2.67E−02	Nucleus
19	IPI:IPI00216691.5	PFN1	Profilin-1	0.62	5.68E−04	Cytoskeleton
20	IPI:IPI00020599.1	CALR	Calreticulin	0.62	1.24E−04	Endoplasmic reticulum
21	IPI:IPI00419237.3	LAP3	Isoform 1 of Cytosol aminopeptidase	0.70	1.66E−02	Cytoplasm
22	IPI:IPI00072377.1	SET	Isoform 1 of Protein SET	0.66	1.28E−02	Endoplasmic reticulum
23	IPI:IPI00872952.1	UQCRH	Ubiquinol-cytochrome c reductase hinge protein, isoform CRA_c	0.66	4.26E−02	Mitochondrial
24	IPI:IPI00219306.1	MAGOH	Protein mago nashi homolog	0.56	5.48E−03	Nucleus
25	IPI:IPI00294739.1	SAMHD1	Isoform 1 of SAM domain and HD domain-containing protein 1	0.71	1.11E−03	Nucleus
26	IPI:IPI00217030.10	RPS4X	40S ribosomal protein S4, X isoform	0.72	2.05E−02	Ribosome
27	IPI:IPI00025252.1	PDIA3	Protein disulfide-isomerase	0.74	1.90E−03	Endoplasmic reticulum
28	IPI:IPI00796366.2	MYL6 cDNA FLJ56329	Highly similar to Myosin light polypeptide 6	0.74	1.40E−02	Cytoskeleton
29	IPI:IPI00744148.2	H2AFY	Isoform 1 of Core histone macro-H2A.1	0.75	5.83E−04	Nucleus
30	IPI:IPI00795292.1	NME2	NME1-NME2 Isoform 3 of Nucleoside diphosphate kinase B	0.75	1.29E−02	Nucleus
31	IPI:IPI00465248.5	ENO1	Isoform alpha-enolase of Alpha-enolase	0.77	7.25E−04	Cytoplasm
32	IPI:IPI00024915.2	PRDX5	Isoform Mitochondrial of Peroxiredoxin-5, mitochondrial	0.64	5.63E−04	Mitochondrial
33	IPI:IPI00419373.1	HNRNPA3	Isoform 1 of Heterogeneous nuclear ribonucleoprotein A3	0.611	3.89E−03	Nucleus
34	IPI:IPI00012011.6	CFL1	Cofilin-1	0.55	6.53E−03	Cytoskeleton
35	IPI:IPI00792011.1	CAPS	Calcyphosin	0.73	4.87E−02	Cytoplasm
36	IPI:IPI00792352.1	RAN	RANP1 26 kDa protein	0.61	2.84E−03	Nucleus
37	IPI:IPI00027462.1	S100A9	Protein S100A9	5.70	6.86E−03	Cytoplasm
38	IPI:IPI00304962.3	COL1A2	Collagen alpha-2(I) chain	1.31	4.60E−03	Extracellular matrix
39	IPI:IPI00479517.2		14 kDa protein	1.34	2.38E−02	Unclassfied
40	IPI:IPI00027107.5	TUFM	Tu translation elongation factor, mitochondrial precursor	1.15	4.99E−02	Mitochondrial
41	IPI:IPI00005198.2	ILF2	Interleukin enhancer-binding factor 2	1.55	3.57E−02	Nucleus
42	IPI:IPI00013895.1	S100A11	Protein S100-A11	1.37	3.90E−02	Cytoplasm
43	IPI:IPI00291006.2	MDH2	Malate dehydrogenase, mitochondrial	1.39	2.78E−03	Mitochondrial
44	IPI:IPI00014053.3	TOMM40	Isoform 1 of Mitochondrial import receptor subunit TOM40 homolog	1.4	1.67E−02	Mitochondrial
45	IPI:IPI00008529.1	RPLP2	60S acidic ribosomal protein P2	1.43	3.27E−02	Ribosome
46	IPI:IPI00604620.3	NCL	Nucleolin	1.43	1.32E−03	Nucleus
47	IPI:IPI00025874.2	RPN1	Dolichyl-diphosphooligosaccharide--protein glycosyltransferase subunit 1 precursor	1.44	3.21E−02	Endoplasmic reticulum
48	IPI:IPI00021812.2	AHNAK	Neuroblast differentiation-associated protein AHNAK	1.46	1.88E−02	Unclassfied
49	IPI:IPI00220362.5	HSPE1	10 kDa heat shock protein, mitochondrial	1.48	2.63E−04	Mitochondrial
50	IPI:IPI00025366.4	CS	Citrate synthase, mitochondrial	1.33	4.53E−02	Mitochondrial
51	IPI:IPI00006865.3	SEC22B	Vesicle-trafficking protein SEC22b	1.51	2.25E−03	Endoplasmic reticulum
52	IPI:IPI00021766.5	RTN4	Isoform 1 of Reticulon-4	1.56	8.80E−03	Endoplasmic reticulum
53	IPI:IPI00013508.5	ACTN1	Alpha-actinin-1	1.59	2.45E−02	Cytoskeleton
54	IPI:IPI00297646.4	COL1A1	Collagen alpha-1(I) chain	1.92	3.16E−07	Extracellular matrix
55	IPI:IPI00386879.1	IGHA1	cDNA FLJ14473 fis, clone MAMMA1001080, highly similar to Homo sapiens SNC73 protein (SNC73) mRNA	1.63	4.29E−03	Unclassfied
56	IPI:IPI00007188.5	SLC25A5	ADP/ATP translocase 2	1.69	3.28E−02	Mitochondrial

Table 1. (*Continued*)

N	Accession	Gene Sym	Protein	Stem cell: Glioma	PVal Stem cell: Glioma	Subcellular location
57	IPI:IPI00794543.1	CALM1;CALM2;CALM3	cDNA FLJ75174, highly similar to Homo sapiens calmodulin 1 (phosphorylase kinase, delta), mRNA	1.74	3.84E−02	Cytoskeleton
58	IPI:IPI00646182.5	ATP1A1	Na+/K+ -ATPase alpha 1 subunit isoform c	1.74	4.08E−04	Plasma membrane
59	IPI:IPI00414696.1	HNRNPA2B1	Isoform A2 of Heterogeneous nuclear ribonucleoproteins A2/B1	1.55	9.59E−03	Nucleus
60	IPI:IPI00011229.1	CTSD	Cathepsin D	1.93	1.44E−02	Lysosome
61	IPI:IPI00014230.1	C1QBP	Complement component 1 Q subcomponent-binding protein, mitochondrial	1.99	2.25E−02	Mitochondrial
62	IPI:IPI00828117.1	CD44	Isoform 5 of CD44 antigen	1.92	1.18E−03	Plasma membrane
63	IPI:IPI00418471.6	VIM	Vimentin	2.4	1.40E−45	Cytoskeleton
64	IPI:IPI00418169.3	ANXA2	Isoform 2 of Annexin A2	1.94	2.70E−04	Cytoskeleton
65	IPI:IPI00183695.9	S100A10	Protein S100-A10	3.38	3.05E−05	Cytoplasm

were killed at day 25, and the xenograft tumors were dissected and weighed.

TISSUE SAMPLES

Tissue samples were provided in the form of tissue microarrays (US Biomax, Inc., Rockville, MD, USA Catalog No. GL722 and GL807). Fifteen of the 50 samples had a GBM (age: 36 ± 17 years; 6 females and 9 males); 20 samples had a WHO grade III astrocytoma (age: 46 ± 11 years; 7 females and 12 males); 10 samples had a WHO grade II astrocytoma (age: 42 ± 12 years; 5 females and 8 males); five samples had a WHO grade I astrocytoma(age: 42 ± 10 years; 1 females and 2 males); eight samples were from normal subjects (age: 41 ± 10 years; 4 females and 4 males). The tissue samples were originated from different donors and each sample had at least two replicates. The glioma tissue sections are from the tumor areas and do not include the adjacent normal tissues.

IMMUNOHISTOCHEMICAL ANALYSIS OF TISSUE MICROARRAYS

Immunohistochemical staining was performed using tissue microarrays. The paraffin-embedded 5 μm arrays were dewaxed in xylene for 10 min and rehydrated through a series of alcohol solutions (100% ethanol twice, 90% ethanol, 70% ethanol, 5 min each) to water. Antigen retrieval was achieved by boiling the arrays in a citrate buffer at pH 6.0. Endogenous peroxidase activity was blocked using 6% H_2O_2. The tissue microarrays were blocked with 2% normal goat serum and incubated with rabbit antihuman S100A9 monoclonal antibody overnight at 4°C. Immunodetection was performed using the EliVision™ plus system (Sigma) according to the manufacturer's instructions. Hematoxylin counterstain was used to visualize nuclei. The S100A9 expression level in each tissue section was assessed in nonnecrotic areas of three separate microscopic fields of view under a magnification of 20× and was represented by the mean of the percentage of S100A9 + cells.

STATISTICAL ANALYSIS

Data were analyzed using GraphPad Prism (version 5.0) (GraphPad Software, La Jolla, CA). Data points in graphs represent the mean ± SD and $P < 0.05$ is considered significant.

RESULTS

INDUCTION OF GLIOMA STEM CELLS

U251 cell became floating neurospheres following cultivation in NSC-medium for 7–10 days. $CD133^+$ glioma stem cells were successfully isolated from the U251 cell-generated neurospheres using CD133 isolation. The ratio of $CD133^+$ glioma stem cells was analyzed using flow cytometry assay. As shown in Figure 1A. When cultured in NSC medium, the CSCs grew in suspension and presented features associated with stem cells, including a sphere-like shape, and the ability to self-renew and differentiate. Immunofluorescent staining for nestin and CD133 was positive in the stem cell (Fig. 1B).

DIFFERENTIATION OF GLIOMA STEM CELLS

The induced glioma stem cells began differentiating after being culturing in DMEM/F12 medium with 10% FBS. After 4 h of culturing

in the differentiation medium, the stem spheres adhered to the well walls, without tumor cells migrating from the spheres, whereas a small proportion of the tumor cells migrated out from the spheres after 24 h in culture. On the day 3, more tumor cells migrated to greater distances and the tumor spheres flattened. On day 7, proliferating tumor cells covered the bottoms of the flasks and masked primary tumor cells. The differentiated cells were positive GFAP staining (Fig. 1C).

PROTEOME DIFFERENCES BETWEEN GLIOMA STEM CELLS AND THEIR DIFFERENTIATED CELLS

Total protein was harvested from the cells as described in the experimental procedures section. The proteins were digested with trypsin, labeled with iTRAQ reagents, and analyzed using tandem mass spectrometry in order generate a profile for the protein levels in glioma stem cells and their differentiated cells. To increase the protein identification coverage and the confidence in the data generated, we prepared and analyzed two biological replicates. Protein from the human U251 glioma cell was labeled in duplicate using mass 113 and 115 isobaric iTRAQ tags, while the stem cell was labeled in duplicate using the mass 114 and 116 isobaric iTRAQ tags. The 114:113 and 116:115 ratios indicate the relative abundance of the proteins from the stem cell line compared to the differentiated progeny. An example is the overall iTRAQ data for the S100A9 protein. The MS/MS spectra for one of its peptides and the relative levels of the iTRAQ tags extracted from the ProteinPilot™ software are shown in Figure 2.

A total of 559 unique proteins were identified with 95% confidence by the ProteinPilot search algorithm against the IPI human protein database v3.41.Although the relative quantification analysis done with the ProteinPilot 2.0 software includes a statistical analysis, most statistical methods used are subject to technical variation. Examination of the average values and the standard deviations for the data from duplicate experiments revealed that the overall variation was less than 30%. This is consistent with the various published and

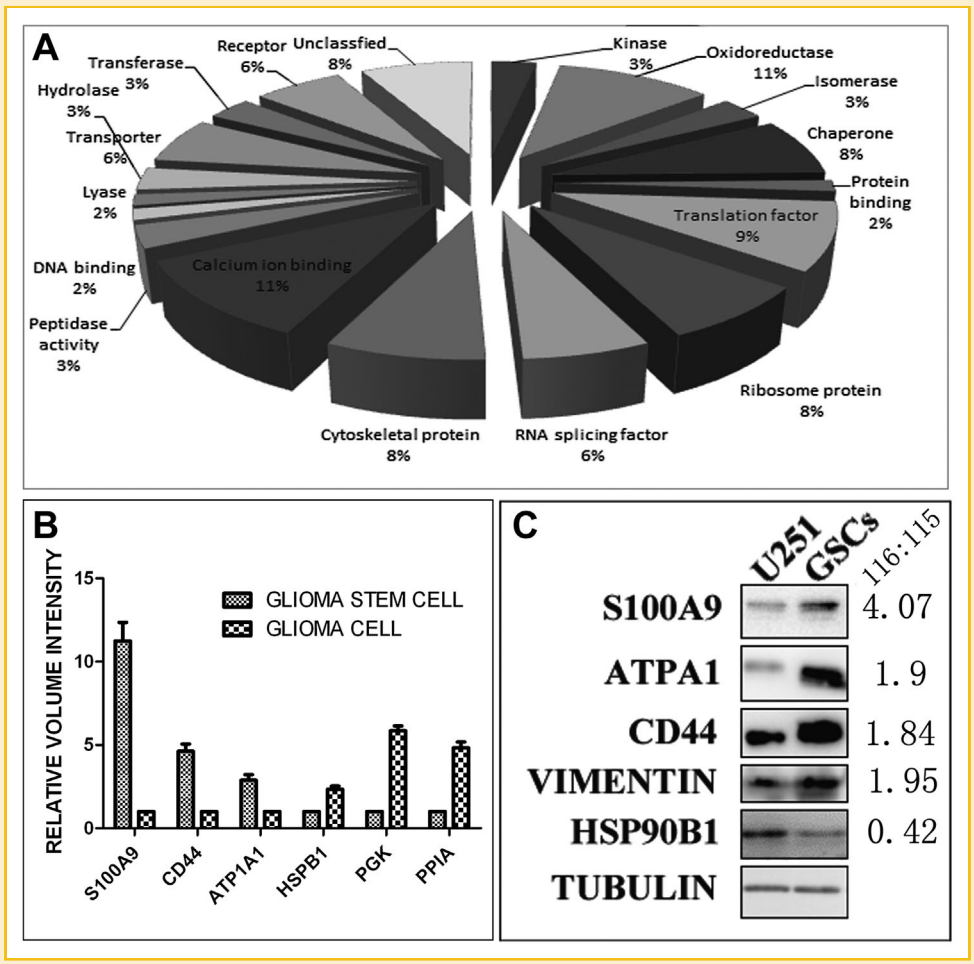

Fig. 3. A: Pie chart showing the various functional categories as a percentage of the 65 differentially expressed proteins according to PANTHER. B: Relative mRNA expression levels of ATP1A1, HSPB1, S100A9, CD44, PPIA, and PGK1 after normalization to 18s RNA levels as determined by real-time RT-qPCR. The glioma U251 stem cells showed obvious up- or down-regulation of mRNA levels compared to the glioma U251 cells; these changes were identical with the protein level changes observed in the iTRAQ analysis. C: Western blot analyses for selected candidate proteins (S100A9, CD44, ATPA1, VIMENTIN, and HSP90B1) in the conditioned medium of glioma U251 cells and glioma U251 stem cells. Total protein stained with Tubulin was included to show relative loading amounts. And 116:115 ratios indicate the relative abundance of the proteins from the stem cell line compared to the differentiated progeny.

unpublished iTRAQ studies. Therefore, we included an additional 1.3-fold change cutoff for all iTRAQ ratios (ratio < 0.77 or > 1.3) for classifying proteins as being up- or down-regulated, resulting in a high and low range of 1.3 (1×1.3)–0.77 (1/1.3), respectively. In other words, proteins with iTRAQ ratios below the low end of the range were considered to be under-expressed, whereas those above the upper end of the range were considered to be over-expressed. Using these classification criteria, we found 65 proteins whose expression levels differed between the glioma stem cell and differentiated cells (Table I).

CLASSIFICATION OF PROTEINS BASED ON MOLECULAR AND CELLULAR FUNCTIONS

In our analysis, we selected 65 proteins as having altered expression in the glioma cell using proteomic techniques. We categorized the proteins based on their functional assignments using PANTHER software (www.pantherdb.org) (Fig. 3A). The proteins provided similar results. The 17 categories of modules and gene ontology terms overlapped for the genes identified as having significant differences based on the proteomics analysis. The molecular functions reported include kinase activity, oxidoreductase activity, isomerase activity, peptidase activity, lyase activity, hydrolase activity, transferase activity, protein binding activity, DNA binding activity, translation factor activity, structural molecules (ribosome and cytoskeleton), chaperone activity, RNA splicing factor activity, calcium ion binding activity, receptor activity, and transporter activity.

VALIDATION OF ITRAQ DATA USING SELECTED CANDIDATES

Based on the importance of the candidate proteins, the availability of commercial antibodies and the degree of differential expression, we selected candidates of interest for further test using Western blot analysis and RT-qPCR. In order to provide original and in-depth insights into glioma stem cell, we selected one candidate, S100A9, for further analysis because it had not previously been reported as being aberrantly expressed in glioma stem cell. We detected a fivefold difference in the protein level of S100A9 expression in glioma stem cells compared to differentiated cell according to iTRAQ data. S100A9′s relationships with several interesting pathways involved in tumor development and progression also highlights the potential importance of this gene. S100A9 is a member of the S100 family, which has been implicated in a Ca^{2+} signaling network and the regulation of numerous intracellular activities, including cell growth, differentiation, migration, adhesion, and enzymatic activity. S100 proteins have been previously detected in acute and chronic inflammation and are regarded as pro-inflammatory cytokines [Hobbs et al., 2003]. Subsequently, it was shown that the differential expression of S100A9 contributes to the development and progression of various types of cancer and that it may be a marker for the growth by malignant tumors. The rest of the proteins are known to be associated with cancer [e.g., CD44, VIM, and Peptidyl-prolyl *cis–trans* isomerase A (PPIA)], to represent emerging drug targets [e.g., heat shock protein (HSP90B1) and (HSPB1)], ATP1A1, and Phosphoglycerate kinase 1 (PGK1). The relative levels of the majority of these proteins in U251 glioma cell versus the stem cell are presented in Figure 3B and C, which show that the differential expression levels of the candidate proteins as detected by RT-qPCR and immunoblotting are largely congruent with those obtained by iTRAQ.

S100A9 IS HIGHLY EXPRESSED IN GLIOMA STEM CELLS

We verified the up-regulation of S100A9 in U251 glioma stem cells and their differentiated stem cells by western blotting. As shown in Figure 4, S100A9 protein were strongly expressed in U251 glioma stem cells, whereas rarely detected in their differentiated progeny. To determine whether S100A9 is also highly expressed in glioma stem cells derived from different cell, we examined its level in CD133+ cells isolated from two glioma cell lines SHG44 and U87. The protein levels of S100A9 were much higher in the glioma stem cells of SHG44 and U87 than their differentiated progeny (Fig. 4).

S100A9 REGULATES GLIOMA STEM CELLS PROLIFERATION IN VITRO AND IN VIVO

To further investigate the effect of S100A9 on glioma growth, glioma stem cell, and SHG44 glioma stem cell was transfected with shRNA-expressing vector to knock down the S100A9 expression. Real time qPCR and Western blot showed that S100A9 expression was markedly decreased in cells transfected with sh- S100A9-1 or sh-S100A9-2 vector compared with cells transfected with sh-NC vector and cells without transfection (U251GSCs-N and SHG44GSCs-N) (Fig. 5A). To investigate the effect of S100A9 knockdown on cell

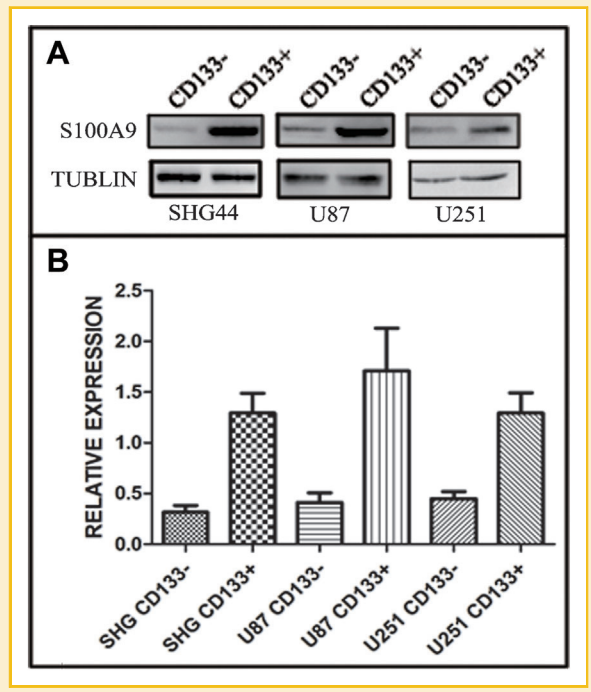

Fig. 4. S100A9 is highly expressed in Glioma stem cells. Expression of S100A9 in three glioma stem cells and their differentiated cells were detected by Western blot (A). Tublin was used as an internal control. The intensity values of S100A9 expression in various cell lines were normalized against those of controls and shown (B).

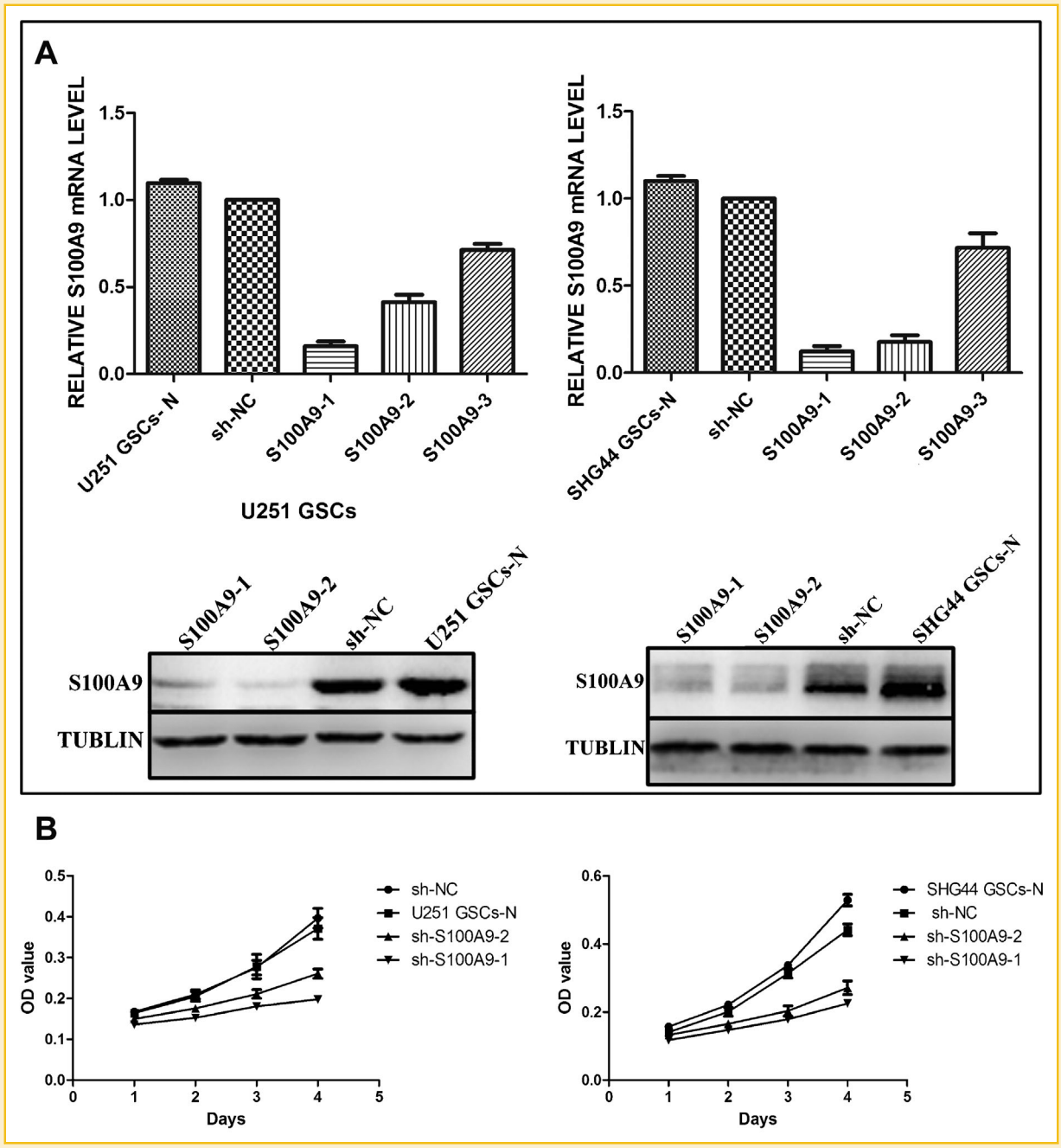

Fig. 5. Tumor cell proliferation assessed by CCK-8assays and tumor xenografts. A: U251 glioma stem cells (1) and SHG44 glioma stem cells (2) were transfected with two vectors expressing different shRNAs silencing S100A9 (*sh-S100A9-1* and *sh-S100A9-2*) or negative control vector (*sh-NC*). Knockdown efficiencies of two independent shRNAs were assessed by real time PCR (upper panel) and Western blot (lower panel). B: Proliferation of the U251 glioma stem cells (1) and SHG44 glioma stem cells (2) stably transfected with sh-S100A9, sh-S100A9-2, and sh-NC were analyzed by CCK-8 assay. The data are expressed as the means ± S.D. from five replicates in each group. C: U251 glioma stem cells (1) and SHG44 glioma stem cells (2) stably transfected with sh-S100A9-1 or sh-NC were injected subcutaneously in the right flank of athymic nude mice (2×10^6 cells/mouse, five mice/group). Tumor volume was monitored at indicated times, and tumor growth curves were plotted (top panel). The data are expressed as the means ± S.D. from five mice in each group. The mice were killed at day 25, and the xenograft tumors were weighed (middle panel) and shown (bottom panel). The data shown are representative of three independent experiments.

proliferation, growth of cells was assessed by CCK-8 assay. As shown in Figure 5B, knockdown of S100A9 obviously decreased proliferation of U251 glioma stem cell and SHG44 glioma stem cell cells cultured in vitro. Furthermore, we evaluated the effect of S100A9 on tumor growth in vivo using a xenograft model. U251 glioma stem cell and SHG44 glioma stem cell transfected with sh- S100A9-1 or sh-NC vector were implanted in nude mice subcutaneously, and tumor size was measured every 5 days. The mice were killed at day 25, and the tumors were dissected and weighed. As shown in Figure 5C, the cells with S100A9 knockdown resulted in slower growing xenografts as

compared with cells with control vector. In 25 days, tumors from S100A9 knockdown cells were on average 60% smaller in weight than tumors from control cells (U251:0.09 vs. 0.3 g, respectively; SHG: 0.63:0.24, $P < 0.05$, *t*-test). The results indicated that the down-regulation of S100A9 expression decreased the growth of glioma cells.

S100A9 IS A TARGET FOR HIGH-GRADE GLIOMAS

Expression levels of S100A9 were assessed immunohistochemically using tissue microarrays containing 50 gliomas of different WHO grades and eight normal subjects. Substantial differences in S100A9 staining were observed between high-grade and low grade gliomas. S100A9 was not detectable in normal brains (Fig. 6A), WHO grade I astrocytomas (Fig. 6B), and most of WHO II astrocytomas (Fig. 6C). In contrast, the expression of S100A9 was dramatically higher in WHO grade III astrocytomas (Fig. 6D) and GBMs (Fig. 6E).

The S100A9 expression level in each tissue section was semiquantitatively represented by the percentage of S100A9 + cells. The relative S100A9 expression levels in normal brains, WHO grade I astrocytomas, WHO grade II astrocytomas, WHO grade III astrocytomas, and GBMs are shown in Figure 6F. All normal brains and WHO grade I astrocytomas showed zero S100A9 levels. In patients with WHO grade II astrocytomas, S100A9 was either not detectable (10 of 13, 77%) or expressed in less than 1% of cells (3 of 13, 23%). As to high-grade gliomas, S100A9 was detectable in all tested samples, with an average S100A9 level of 39.6% for WHO grade III astrocytomas (range: 22.4–58.2%; n = 19) and 42.9% for GBMs (range: 25.6–60.5%; n = 15). No significant difference in S100A9 expression was observed between grade I and grade II astrocytomas ($P > 0.05$), neither was there between grade III astrocytomas and GBM ($P > 0.05$). However, the expression levels of S100A9 in high-grade gliomas were significantly higher than in low grade gliomas ($P < 0.05$). As S100A9 was highly expressed in high-grade gliomas but it was almost not expressed in low grade gliomas and normal brains, S100A9 may serve as a target for high-grade gliomas.

DISCUSSION

In the present study we have used a proteomics approach to identify potential regulators of the cancer stem cell in glioma. We identified

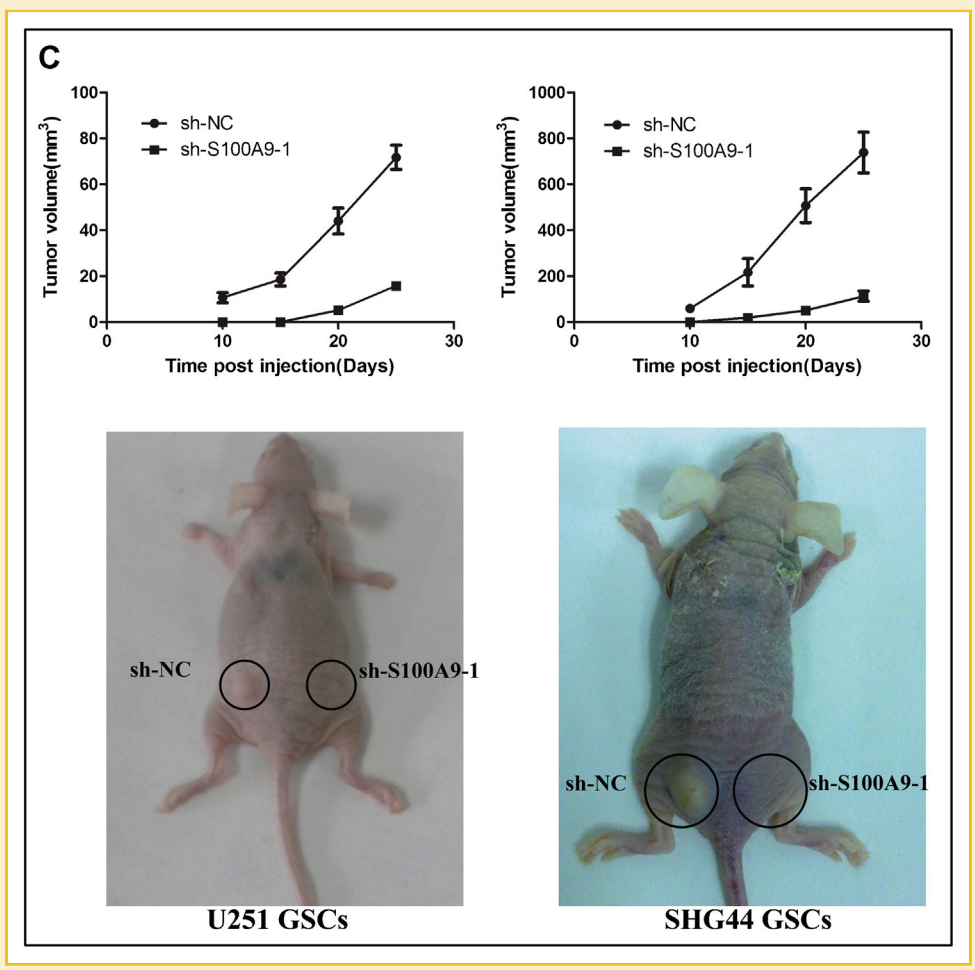

Fig. 5 Continued.

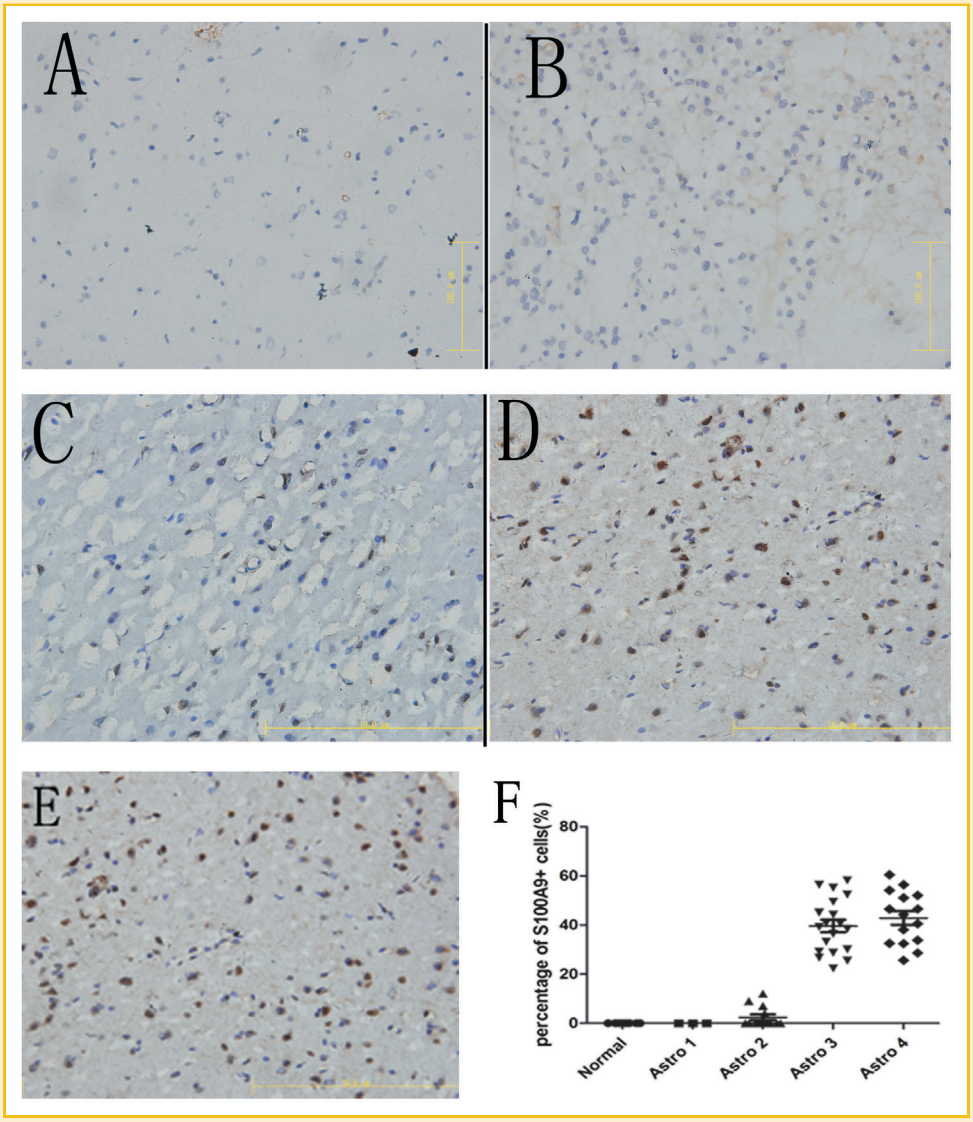

Fig. 6. Immunohistochemical staining for human S100A9 in different grades of astrocytomas and normal brains. Paraffin-embedded tissue microarrays were stained using an anti-human S100A9 antibody. S100A9 was not detected in normal brain (A), astrocytoma WHO grade I (B), and diffuse astrocytoma WHO grade II (C). In contrast, moderate or strong staining for S100A9 was observed in anaplastic astrocytoma WHO grade III (D) and GBM WHO grade IV (E). Hematoxylin counterstain was used to visualize nuclei. Scale bar, 100 μm. F: Scatter plot of S100A9 expression levels in n = 50 patients with different grades of astrocytomas and n = 8 normal subjects. The S100A9 expression level of each tissue sample was represented by the percentage of S100A9 + cells. Each point corresponds to the S100A9 expression level of a single sample. S100A9 expression levels were significantly elevated in patients with high-grade astrocytomas (WHO grade III and IV). Astro 1 represents astrocytoma WHO grade I; Astro 2 represents diffuse astrocytoma (WHO grade II); Astro 3 represents anaplastic astrocytoma (WHO grade III); GBM represents glioblastoma multiforme (WHO grade IV).

known (S100A9) and novel factors enriched in cancer stem cell cultures when compared with stably differentiated tumor cells. Interestingly, PANTHER software revealed that calcium-binding proteins are significantly enriched in glioma stem cell when compared with differentiated tumor cells. Future work should reveal the function of these proteins in the maintenance of glioma stem cells.

Importantly, CSCs were also characterized by high expression of a set of proliferation proteins, the most prominent of which was S100A9. S100A9 deletion is associated with tumor growth in vivo and vitro studies. Furthermore, S100A9 deletion promotes p53 stabilization and caspase 3 activation [Li et al., 2009b].

Our data show that specifically glioma stem cell cultures display increased growth and that S100A9 is an important mediator of growth. S100A9 belongs to the family of S100 proteins, which are calcium-binding cytosolic molecules characterized by a conserved EF-hand motif. There are presently 20 known members of the S100 family, and the genes encoding most of them are located in a cluster on chromosome 1q21 in humans, where several chromosomal abnormalities have been linked with neoplasia [Petersen et al., 2000; Goeze et al., 2002; Knosel et al., 2002; Jee et al., 2003; Koon et al., 2004; Sy et al., 2004, 2005; Moinzadeh et al., 2005]. S100 proteins mediate various cellular processes including cell growth,

differentiation, cell migration, and cell adhesion [Kerkhoff et al., 1999; Li et al., 2004; Li and Bresnick, 2006]. In addition, the role of S100 proteins in malignant tissues has been studied for several years. To date, S100A2, S100A4, S100A6, S100A7, S100A11, S100P, and S100B have all been reported to associate with human cancers [Heizmann et al., 2002; Marenholz et al., 2004]. Little is known about the clinical role of S100A9 in cancer, our results are in line with previous studies showing that CSCs express high levels of anti-apoptotic proteins and resist apoptotic stimuli.

Because S100 play an important role in tumor maintenance and growth they represent attractive targets for targeted therapy. Furthermore, S100 are highly expressed in several cancer tissues. S100A9 forms a heterodimer with S100A8, and the S100A8/A9 complex is known to be associated with leukocyte adhesion and transendothelial migration [Hobbs et al., 2003; Manitz et al., 2003]. In addition, S100A9 was recently reported to be expressed in breast cancer, gastric cancer, prostate cancer, hepatocellular carcinoma, and lung cancer [Arai et al., 2000, 2001, 2008; El-Rifai et al., 2002; Hermani et al., 2005; Moon et al., 2008], suggesting that S100A8/S100A9 promotes inflammatory responses in infections and is a potent amplifier of inflammation in autoimmunity, cancer development, and tumor spreading and S100A9 may have an important role in cancer. S100A8/A9 interacts with RAGE and carboxylated glycans in colon tumor cells and promotes activation of MAPK and NF-κB signaling pathways. Mice lacking S100A9 show significant reduced tumor incidence, growth and metastasis, reduced chemokine levels, and reduced infiltration of CD11b(+)Gr1(+) cells within tumors and premetastatic organs [Ichikawa et al., 2011].

Based on the data presented here we propose that targeting S100A9 by RNAi or by novel specific S100A9 inhibitors may therefore be effective in anticancer. This may help eradicating the cancer stem cell fraction in glioma.

ACKNOWLEDGMENTS

This work was supported by the National Natural Science Foundation of China (No.30801348, 30870723), Program for Changjiang Scholars, and Innovative Research Team in University No. IRT 0872.

REFERENCES

Arai K, Yamada T, Nozawa R. 2000. Immunohistochemical investigation of migration inhibitory factor-related protein (MRP)-14 expression in hepatocellular carcinoma. Med Oncol 17:183–188.

Arai K, Teratani T, Nozawa R, Yamada T. 2001. Immunohistochemical investigation of S100A9 expression in pulmonary adenocarcinoma: S100A9 expression is associated with tumor differentiation. Oncol Rep 8:591–596.

Arai K, Takano S, Teratani T, Ito Y, Yamada T, Nozawa R. 2008. S100A8 and S100A9 overexpression is associated with poor pathological parameters in invasive ductal carcinoma of the breast. Curr Cancer Drug Targets 8:243–252.

Bao S, Wu Q, McLendon RE, Hao Y, Shi Q, Hjelmeland AB, Dewhirst MW, Bigner DD, Rich JN. 2006. Glioma stem cells promote radioresistance by preferential activation of the DNA damage response. Nature 444:756–760.

Bijian K, Mlynarek AM, Balys RL, Jie S, Xu Y, Hier MP, Black MJ, Di FMR, LaBoissiere S, Alaoui-Jamali MA. 2009. Serum proteomic approach for the identification of serum biomarkers contributed by oral squamous cell carcinoma and host tissue microenvironment. J Proteome Res 8:2173–2185.

Bouchal P, Roumeliotis T, Hrstka R, Nenutil R, Vojtesek B, Garbis SD. 2009. Biomarker discovery in low-grade breast cancer using isobaric stable isotope tags and two-dimensional liquid chromatography-tandem mass spectrometry (iTRAQ-2DLC–MS/MS) based quantitative proteomic analysis. J Proteome Res 8:362–373.

Chaerkady R, Harsha HC, Nalli A, Gucek M, Vivekanandan P, Akhtar J, Cole RN, Simmers J, Schulick RD, Singh S, Torbenson M, Pandey A, Thuluvath PJ. 2008. A quantitative proteomic approach for identification of potential biomarkers in hepatocellular carcinoma. J Proteome Res 7:4289–4298.

El-Rifai W, Moskaluk CA, Abdrabbo MK, Harper J, Yoshida C, Riggins GJ, Frierson HF, Jr. Powell SM. 2002. Gastric cancers overexpress S100A calcium-binding proteins. Cancer Res 62:6823–6826.

Eriksson H, Lengqvist J, Hedlund J, Uhlen K, Orre LM, Bjellqvist B, Persson B, Lehtio J, Jakobsson PJ. 2008. Quantitative membrane proteomics applying narrow range peptide isoelectric focusing for studies of small cell lung cancer resistance mechanisms. Proteomics 8:3008–3018.

Eyler CE, Wu Q, Yan K, MacSwords JM, Chandler-Militello D, Misuraca KL, Lathia JD, Forrester MT, Lee J, Stamler JS, Goldman SA, Bredel M, McLendon RE, Sloan AE, Hjelmeland AB, Rich JN. 2011. Glioma stem cell proliferation and tumor growth are promoted by nitric oxide synthase-2. Cell 146:53–66.

Fan X, Khaki L, Zhu TS, Soules ME, Talsma CE, Gul N, Koh C, Zhang J, Li YM, Maciaczyk J, Nikkhah G, Dimeco F, Piccirillo S, Vescovi AL, Eberhart CG. 2010. NOTCH pathway blockade depletes CD133-positive glioblastoma cells and inhibits growth of tumor neurospheres and xenografts. Stem Cells 28:5–16.

Galli R, Binda E, Orfanelli U, Cipelletti B, Gritti A, De Vitis S, Fiocco R, Foroni C, Dimeco F, Vescovi A. 2004. Isolation and characterization of tumorigenic, stem-like neural precursors from human glioblastoma. Cancer Res 64:7011–7021.

Glen A, Gan CS, Hamdy FC, Eaton CL, Cross SS, Catto JW, Wright PC, Rehman I. 2008. iTRAQ-facilitated proteomic analysis of human prostate cancer cells identifies proteins associated with progression. J Proteome Res 7:897–907.

Goeze A, Schluns K, Wolf G, Thasler Z, Petersen S, Petersen I. 2002. Chromosomal imbalances of primary and metastatic lung adenocarcinomas. J Pathol 196:8–16.

Guryanova OA, Wu Q, Cheng L, Lathia JD, Huang Z, Yang J, MacSwords J, Eyler CE, McLendon RE, Heddleston JM, Shou W, Hambardzumyan D, Lee J, Hjelmeland AB, Sloan AE, Bredel M, Stark GR, Rich JN, Bao S. 2011. Nonreceptor tyrosine kinase BMX maintains self-renewal and tumorigenic potential of glioblastoma stem cells by activating STAT3. Cancer Cell 19:498–511.

Heizmann CW, Fritz G, Schafer BW. 2002. S100 proteins: structure, functions and pathology. Front Biosci 7:d1356–d1368.

Hermani A, Hess J, De Servi B, Medunjanin S, Grobholz R, Trojan L, Angel P, Mayer D. 2005. Calcium-binding proteins S100A8 and S100A9 as novel diagnostic markers in human prostate cancer. Clin Cancer Res 11:5146–5152.

Hobbs JA, May R, Tanousis K, McNeill E, Mathies M, Gebhardt C, Henderson R, Robinson MJ, Hogg N. 2003. Myeloid cell function in MRP-14 (S100A9) null mice. Mol Cell Biol 23:2564–2576.

Ichikawa M, Williams R, Wang L, Vogl T, Srikrishna G. 2011. S100A8/A9 activate key genes and pathways in colon tumor progression. Mol Cancer Res 9:133–148.

Jee KJ, Gong G, Ahn SH, Park JM, Knuutila S. 2003. Gain in 1q is a common abnormality in phyllodes tumours of the breast. Anal Cell Pathol 25:89–93.

Kerkhoff C, Klempt M, Kaever V, Sorg C. 1999. The two calcium-binding proteins, S100A8 and S100A9, are involved in the metabolism of arachidonic acid in human neutrophils. J Biol Chem 274:32672–32679.

Knosel T, Petersen S, Schwabe H, Schluns K, Stein U, Schlag PM, Dietel M, Petersen I. 2002. Incidence of chromosomal imbalances in advanced colorectal carcinomas and their metastases. Virchows Arch 440:187–194.

Koon N, Zaika A, Moskaluk CA, Frierson HF, Knuutila S, Powell SM, El-Rifai W. 2004. Clustering of molecular alterations in gastroesophageal carcinomas. Neoplasia 6:143–149.

Li ZH, Bresnick AR. 2006. The S100A4 metastasis factor regulates cellular motility via a direct interaction with myosin-IIA. Cancer Res 66:5173–5180.

Li C, Zhang F, Lin M, Liu J. 2004. Induction of S100A9 gene expression by cytokine oncostatin M in breast cancer cells through the STAT3 signaling cascade. Breast Cancer Res Treat 87:123–134.

Li C, Chen H, Ding F, Zhang Y, Luo A, Wang M, Liu Z. 2009a. A novel p53 target gene, S100A9, induces p53-dependent cellular apoptosis and mediates the p53 apoptosis pathway. Biochem J 422(2):363–372.

Li Z, Bao S, Wu Q, Wang H, Eyler C, Sathornsumetee S, Shi Q, Cao Y, Lathia J, McLendon RE, Hjelmeland AB, Rich JN. 2009b. Hypoxia-inducible factors regulate tumorigenic capacity of glioma stem cells. Cancer Cell 15:501–513.

Liu G, Yuan X, Zeng Z, Tunici P, Ng H, Abdulkadir IR, Lu L, Irvin D, Black KL, Yu JS. 2006. Analysis of gene expression and chemoresistance of CD133+ cancer stem cells in glioblastoma. Mol Cancer 5:67.

Manitz MP, Horst B, Seeliger S, Strey A, Skryabin BV, Gunzer M, Frings W, Schonlau F, Roth J, Sorg C, Nacken W. 2003. Loss of S100A9 (MRP14) results in reduced interleukin-8-induced CD11b surface expression, a polarized microfilament system, and diminished responsiveness to chemoattractants in vitro. Mol Cell Biol 23:1034–1043.

Marenholz I, Heizmann CW, Fritz G. 2004. S100 proteins in mouse and man: from evolution to function and pathology (including an update of the nomenclature). Biochem Biophys Res Commun 322:1111–1122.

Moinzadeh P, Breuhahn K, Stutzer H, Schirmacher P. 2005. Chromosome alterations in human hepatocellular carcinomas correlate with aetiology and histological grade–results of an explorative CGH meta-analysis. Br J Cancer 92:935–941.

Moon A, Yong HY, Song JI, Cukovic D, Salagrama S, Kaplan D, Putt D, Kim H, Dombkowski A, Kim HR. 2008. Global gene expression profiling unveils S100A8/A9 as candidate markers in H-ras-mediated human breast epithelial cell invasion. Mol Cancer Res 6:1544–1553.

Ohgaki H, Dessen P, Jourde B, Horstmann S, Nishikawa T, Di PPL, Burkhard C, Schuler D, Probst-Hensch NM, Maiorka PC, Baeza N, Pisani P, Yonekawa Y, Yasargil MG, Lutolf UM, Kleihues P. 2004. Genetic pathways to glioblastoma: a population-based study. Cancer Res 64:6892–6899.

Petersen S, Aninat-Meyer M, Schluns K, Gellert K, Dietel M, Petersen I. 2000. Chromosomal alterations in the clonal evolution to the metastatic stage of squamous cell carcinomas of the lung. Br J Cancer 82:65–73.

Piccirillo SG, Reynolds BA, Zanetti N, Lamorte G, Binda E, Broggi G, Brem H, Olivi A, Dimeco F, Vescovi AL. 2006. Bone morphogenetic proteins inhibit the tumorigenic potential of human brain tumour-initiating cells. Nature 444:761–765.

Pierce A, Unwin RD, Evans CA, Griffiths S, Carney L, Zhang L, Jaworska E, Lee CF, Blinco D, Okoniewski MJ, Miller CJ, Bitton DA, Spooncer E, Whetton AD. 2008. Eight-channel iTRAQ enables comparison of the activity of six leukemogenic tyrosine kinases. Mol Cell Proteomics 7:853–863.

Reardon DA, Rich JN, Friedman HS, Bigner DD. 2006. Recent advances in the treatment of malignant astrocytoma. J Clin Oncol 24:1253–1265.

Reya T, Morrison SJ, Clarke MF, Weissman IL. 2001. Stem cells, cancer, and cancer stem cells. Nature 414:105–111.

Ross PL, Huang YN, Marchese JN, Williamson B, Parker K, Hattan S, Khainovski N, Pillai S, Dey S, Daniels S, Purkayastha S, Juhasz P, Martin S, Bartlet-Jones M, He F, Jacobson A, Pappin DJ. 2004. Multiplexed protein quantitation in Saccharomyces cerevisiae using amine-reactive isobaric tagging reagents. Mol Cell Proteomics 3:1154–1169.

Singh SK, Hawkins C, Clarke ID, Squire JA, Bayani J, Hide T, Henkelman RM, Cusimano MD, Dirks PB. 2004. Identification of human brain tumour initiating cells. Nature 432:396–401.

Sy SM, Wong N, Lee TW, Tse G, Mok TS, Fan B, Pang E, Johnson PJ, Yim A. 2004. Distinct patterns of genetic alterations in adenocarcinoma and squamous cell carcinoma of the lung. Eur J Cancer 40:1082–1094.

Sy SM, Wong N, Lai PB, To KF, Johnson PJ. 2005. Regional over-representations on chromosomes 1q, 3q and 7q in the progression of hepatitis B virus-related hepatocellular carcinoma. Mod Pathol 18:686–692.

Visvader JE, Lindeman GJ. 2008. Cancer stem cells in solid tumours: accumulating evidence and unresolved questions. Nat Rev Cancer 8:755–768.

Zhu TS, Costello MA, Talsma CE, Flack CG, Crowley JG, Hamm LL, He X, Hervey-Jumper SL, Heth JA, Muraszko KM, DiMeco F, Vescovi AL, Fan X. 2011. Endothelial cells create a stem cell niche in glioblastoma by providing NOTCH ligands that nurture self-renewal of cancer stem-like cells. Cancer Res 71:6061–6072.